

Solid-State ^{15}N NMR Chemical Shift Anisotropy of Histidines: Experimental and Theoretical Studies of Hydrogen Bonding[†]

Yufeng Wei,[‡] Angel C. de Dios,[§] and Ann E. McDermott^{*‡}

Contribution from the Department of Chemistry, Columbia University, New York, New York 10027, and Department of Chemistry, Georgetown University, Washington, D.C. 20057

Received June 8, 1999. Revised Manuscript Received August 11, 1999

Abstract: The principal values of the ^{15}N chemical shift tensors of crystalline histidine and histidine-containing peptides have been measured to document for the first time the systematic trends in values of imidazole CSA with changes in hydrogen bonds. NMR measurement of imidazole groups, both ^{15}N and ^1H , is a key method for studying strong and $\text{p}K_{\text{a}}$ -matched hydrogen bonds and their roles in enzymes, but appropriate model compound data and calculations are largely lacking in the literature. On the basis of this database of experimental values for imidazole groups interacting with carboxylate hydrogen-bonding partners, and of ab initio calculations for similar structures, a correlation was found between the ^{15}N δ_{22} tensor value and the hydrogen bond length for cationic species. As the hydrogen bond distance decreases, the δ_{22} tensor value shifts downfield. No correlation was found between the ^{15}N CSA tensor elements of neutral imidazole and the corresponding hydrogen bond distance, probably because the range of hydrogen-bonding distances in our compounds is limited (~ 0.05 Å) and because this functionality is not involved in nearly $\text{p}K_{\text{a}}$ -matched hydrogen bonds. Ab initio ^{15}N shielding calculations for an imidazolium acetate (cationic) model showed general agreement with the trends in the experimental results, although the breadths of the calculated CSA tensors are systematically larger than those determined experimentally, and the variation in the calculated CSA tensor values is somewhat smaller than that obtained experimentally.

Histidine is a key residue in enzymatic catalysis. It can act as a general acid or base to protonate or deprotonate the substrates; it apparently also participates in hydrogen bonding to stabilize transition states for several enzymes such as serine proteases, enolizing enzymes (triosephosphate isomerase and citrate synthase as examples), and hydrolytic enzymes (such as ribonuclease A). It has been proposed that neutral imidazole acts as general acid to protonate the substrate, and becomes transiently anionic in the case of triosephosphate isomerase,¹ and that “low-barrier” hydrogen bonds between imidazole ring nitrogens and the substrates in these enzymes^{2,3} lower the transition-state energy. Arguably, NMR chemical shifts have been the most insightful tool for studying hydrogen bonds in enzyme active sites. Histidine has been extensively characterized by ^{15}N NMR spectroscopy both in solution and in the solid state. The isotropic shift is a good indicator of the protonation state, and can provide information concerning hydrogen bonding. Bachovchin and co-workers systematically classified isotropic chemical shifts of imidazole ring nitrogens according to their protonation states.^{4,5} To our knowledge, no systematic database

of ^{15}N and ^1H shifts for imidazoles with varied hydrogen-bonding environments has yet been reported.

In the context of understanding chemical trends underlying variation in chemical shielding, solid-state NMR measurements of crystalline compounds have the advantage that direct comparison with high-quality X-ray and sometimes even neutron diffraction coordinates is possible. Furthermore, full tensorial information is obtained, which is often more indicative of the nonbonded interactions. Anisotropic chemical shifts have the potential to reveal more detail about the hydrogen-bonding interactions. For example, chemical shift anisotropy has been used to study the hydrogen-bonding property of carboxyl groups^{6,7} and amides.⁸ For the case of carboxyl, it was shown that the three tensor elements reveal completely different facets: one responds to the ionization state, another responds to the hydrogen bond distance in the syn direction, and the third is constant unless there is motion of the group. Recent studies of citrate synthase applied ^{13}C CSA tensors to understand enzymatic inhibited complexes.⁹ For the case of the ^{15}N in imidazole, the orientations of the CSA and principal values have been measured using single-crystal methods, and the molecular orientations of the tensors for the imidazole ring in L-histidine monohydrochloride monohydrate have been shown to be essentially along the molecular symmetric axes:¹⁰ δ_{11} is nearly along the N–H vector, δ_{33} is almost perpendicular to the plane

* To whom correspondence should be addressed.

[†] Abbreviations: NMR, nuclear magnetic resonance; CSA, chemical shift anisotropy; GIAO, gauge including atomic orbital; IGLO, individualized gauge for localized orbital; SCF, self-consistent field; DFT, density functional theory; SOS-DFPT, sum-over-state density functional perturbation theory; CSD, Cambridge Structural Database.

[‡] Columbia University.

[§] Georgetown University.

(1) Lodi, P. J.; Knowles, J. R. *Biochemistry* **1991**, *30*, 6948–6956.

(2) Cleland, W. W.; Kreevoy, M. M. *Science* **1994**, *264*, 1887–1890.

(3) Frey, P. A.; Whitt, S. A.; Tobin, J. B. *Science* **1994**, *264*, 1927–1930.

(4) Bachovchin, W. W. *Biochemistry* **1986**, *25*, 7751–7759.

(5) Smith, S. O.; Farr-Jones, S.; Griffin, R. G.; Bachovchin, W. W. *Science* **1989**, *244*, 961–964.

(6) Gu, Z.; McDermott, A. *J. Am. Chem. Soc.* **1993**, *115*, 4282–4285.

(7) Gu, Z.; Zambrano, R.; McDermott, A. *J. Am. Chem. Soc.* **1994**, *116*, 6368–6372.

(8) Shoji, A.; Ando, S.; Kuroki, S.; Ando, I.; Webb, G. A. *Annu. Rep. NMR Spectrosc.* **1993**, *26*, 55–98.

(9) Gu, Z.; Drueckhammer, D. G.; Kurz, L.; Liu, K.; Martin, D. P.; McDermott, A. *Biochemistry* **1999**, *38*, 8022–8031.

(10) Harbison, G.; Herzfeld, J.; Griffin, R. G. *J. Am. Chem. Soc.* **1981**, *103*, 4752–4754.

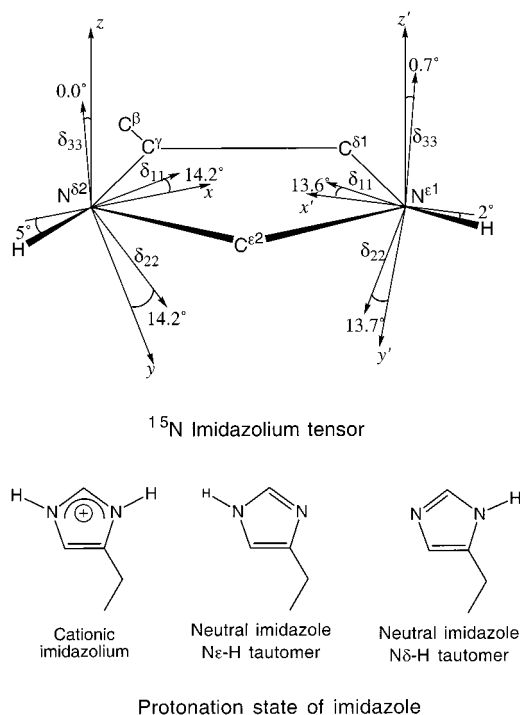


Figure 1. Top: Molecular orientation of the ^{15}N imidazole tensors. The xyz coordinate system was chosen so that z is perpendicular to the ring, x bisects the CNC angle, and y is orthogonal to these orientations. The principal axes of the shift tensor lie near these molecular symmetry directions. Adapted from G. Harbison, J. Herzfeld, and R. G. Griffin (*J. Am. Chem. Soc.* **1981**, *103*, 4752–4754). Bottom: Three types of protonation states for the imidazole ring.

of the imidazole ring for both nitrogens, and δ_{22} is approximately orthogonal to the N–H direction and in the plane of the imidazole ring (Figure 1, top). Roberts et al. reported dipolar and chemical shift anisotropy for L-His·HCl·H₂O, and compared the N^ε–H bond length from NMR spectroscopy and neutron diffraction.¹¹ Ramamoorthy et al. determined ^{15}N chemical shift tensors and orientations of histidine by analyzing the three-dimensional powder pattern which correlates chemical shifts of ^1H and ^{15}N and the ^1H – ^{15}N dipolar coupling, and good agreement with the single-crystal experiment was achieved.¹²

CSA tensors can be studied in a variety of ways besides solid-state methods. Efforts to extract tensorial information from solution NMR measurements have met with varied success; these efforts have focused mainly on the amide functionality and may not often be applicable to the imidazole moiety. ^{15}N CSA can be measured in principle by solution NMR using the CSA/dipolar cross-correlated relaxation technique.^{13–15} A model-independent method of analysis of NMR relaxation data was also demonstrated using human ubiquitin.^{16,17} Whether tensorial values for the shift, and their orientations, can be determined with adequate precision by these methods for chemical trends

(11) Roberts, J. E.; Harbison, G. S.; Munowitz, M. G.; Herzfeld, J.; Griffin, R. G. *J. Am. Chem. Soc.* **1987**, *109*, 4163–4169.

(12) Ramamoorthy, A.; Wu, C. H.; Opella, S. J. *J. Am. Chem. Soc.* **1997**, *119*, 10479–10486.

(13) Tjandra, N.; Szabo, A.; Bax, A. *J. Am. Chem. Soc.* **1996**, *118*, 6986–6991.

(14) Tessari, M.; Mulder, F. A. A.; Boelens, R.; Vuister, G. W. *J. Magn. Reson.* **1997**, *127*, 128–133.

(15) Tessari, M.; Vis, H.; Boelens, R.; Kaptein, R.; Vuister, G. W. *J. Am. Chem. Soc.* **1997**, *119*, 8985–8990.

(16) Fushman, D.; Cowburn, D. *J. Am. Chem. Soc.* **1998**, *120*, 7109–7110.

(17) Fushman, D.; Tjandra, N.; Cowburn, D. *J. Am. Chem. Soc.* **1998**, *120*, 10947–10952.

to be discerned remains under debate (Kroncke, Rance, and Palmer, *J. Am. Chem. Soc.* in press).

Of course NMR chemical shift tensors have gradually risen to one of the most popular topics for theoretical chemists, and ab initio methods have already reached the stage at which calculated isotropic shifts have approached experimental ones within the precision of the experiment.¹⁸ Experimental tensor shifts provide rigorous tests for quantum mechanical methods; thus, back-to-back comparisons are particularly important. ^{15}N CSA tensors for imidazoles have been previously compared with theoretical results, and the orientations of tensors were also calculated in terms of electron orbitals with marked success.¹⁹ A recent theoretical study suggests that amide ^{15}N shielding tensors have a very specific dependence on hydrogen bonding, as well as on the secondary structure or backbone torsional state.²⁰

However, trends in imidazole CSA values as the hydrogen bond changes have not been reported in calculations or experimental databases, to our knowledge. Thus, the central point of interest to enzymologists has not yet been calibrated and reported in the literature. With these considerations in mind, we have prepared databases of chemical shift tensor values that will be useful for studies of imidazole groups in enzymes. In this study, we report ^{15}N chemical shift anisotropy for a variety of crystalline histidine and histidine-containing peptides at natural abundance. We compare our experimental values to those obtained through ab initio calculations. Two companion studies are also of interest in this context. We have recently reported a solid-state ^1H chemical shift database for histidines, and the hydrogen-bonding effects on the chemical shift trends were discussed in terms of $\text{p}K_{\text{a}}$ matching conditions and crystallographic distances.²¹ Variations in the N–H (covalent) bond lengths are likely to underlie the trends in both chemical shift values. Therefore, a study of N–H bond variations in histidine using solid-state heteronuclear dipolar recoupling techniques^{22,23} is also underway.

Materials and Methods

Sample Preparation. Natural abundance L-histidine, DL-histidine, and peptides were purchased from Sigma Chemical Co. The crystal structures were retrieved from the Cambridge Structural Database (CSD).^{24–26} Crystallization of samples was accomplished according to the crystallographic studies (L-carnosine,²⁷ L-His-L-Leu,²⁸ L-histidine

(18) Sitkoff, D.; Case, D. A. *Prog. NMR Spectrosc.* **1998**, *32*, 165–190.

(19) Solum, M. S.; Altmann, K. L.; Strohmeier, M.; Berges, D. A.; Zhang, Y.; Facelli, J. C.; Pugmire, R. J.; Grant, D. M. *J. Am. Chem. Soc.* **1997**, *119*, 9804–9809.

(20) Walling, A. E.; Pargas, R. E.; de Dios, A. C. *J. Phys. Chem. A* **1997**, *101*, 7299–7303.

(21) Wei, Y.; McDermott, A. E. In *Modeling NMR Chemical Shifts: Gaining Insights into Structure and Environment*; Facelli, J., de Dios, A. C., Eds.; American Chemical Society: Washington, DC, 1999; 177–193.

(22) Hong, M.; Gross, J. D.; Rienstra, C. M.; Griffin, R. G.; Kumashiro, K. K.; Schmidt-Rohr, K. *J. Magn. Reson.* **1997**, *129*, 85–92.

(23) Hong, M.; Gross, J. D.; Griffin, R. G. *J. Phys. Chem. B* **1997**, *101*, 5869–5874.

(24) Allen, F. H.; Bellard, S.; Brice, M. D.; Cartwright, B. A.; Doubleday, A.; Higgs, H.; Hummelink, T.; Hummelink-Peters, B. G.; Kennard, O.; Motherwell, W. D. S.; Rodgers, J. R.; Watson, D. G. *Acta Crystallogr.* **1979**, *B35*, 2331–2339.

(25) Allen, F. H.; Kennard, O.; Taylor, R. *Acc. Chem. Res.* **1983**, *16*, 146–153.

(26) Allen, F. H.; Kennard, O. *Chem. Des. Automat. News* **1993**, *8*, 1, 31–37.

(27) Itoh, H.; Yamane, T.; Ashida, T. *Acta Crystallogr.* **1977**, *B33*, 2959–2961.

(28) Krause, J. A.; Baures, P. W.; Eggleston, D. S. *Acta Crystallogr.* **1993**, *B49*, 123–130.

Table 1. ¹⁵N Chemical Shift Anisotropy (ppm) of Histidines and Crystallographic Hydrogen-Bonding Data

			¹⁵ N CSA ^a				N···X/Å	CSD refcode	
			δ _{iso}	δ ₁₁	δ ₂₂	δ ₃₃			
neutral species	L-carnosine	N ^ε -H	168.4	262.7	176.1	66.3	2.698	BALHIS01	
		N ^δ ···NH ₃	247.1	400.1	309.7	31.5	2.886		
	L-His-L-Leu	N ^δ -H	174.3	278.1	200.0	44.7	2.713	JUKMOR	
		N ^ε ···NH ₃	249.7	346.7	337.8	64.6	2.850		
	L-histidine (monoclinic)	L-histidine (orthorhombic)	N ^ε -H	168.5	260.3	176.2	69.0	2.733	LHISTD02
			N ^δ ···NH ₃	246.7	361.8	330.1	48.6	2.75	
L-histidine (orthorhombic)	L-histidine (orthorhombic)	N ^ε -H	168.3	253.8	181.4	69.8	2.752	LHISTD13	
		N ^δ ···NH ₃	246.5	392.0	313.8	33.9	2.779		
cationic species	DL-histidine hydrochloride dihydrate	N ^ε -H	173.1	263.6	203.1	52.6	2.726	DCHIST	
		N ^δ -H···Cl ⁻	173.1	263.6	203.1	52.6	3.11		
	L-histidine perchlorate	N ^ε -H···ClO ₄ ⁻	168.3	261.8	202.6	40.7	2.933	GASKAM	
		N ^δ -H	164.6	261.7	187.9	44.3	3.037		
	L-histidine hydrochloride monohydrate	N ^ε -H	172.3	265.0	195.0	58.4	2.830	HISTCM12	
		N ^δ -H	185.9	268.6	222.8	66.3	2.642		
	L-histidine hydrogen oxalate	N ^ε -H	184.2	268.6	228.0	55.9	2.627	RARXOX	
		N ^δ -H	174.3	272.9	186.2	63.7	2.910		
	L-histidine glycolate	L-histidine glycolate (unresolved)	N ^ε -H	179.8	278.6	211.1	49.7	2.651	TEJWAG
								2.704	

^a ±5 ppm for CSA elements, ±0.2 ppm for isotropic shifts.

monoclinic form,²⁹ L-histidine orthorhombic form,³⁰ DL-histidine hydrochloride monohydrate,³¹ L-histidine perchlorate,³² L-histidine hydrochloride monohydrate,³³ L-histidine oxalate,³⁴ Gly-L-His hydrochloride dihydrate,³⁵ L-histidine glycolate³⁶). Some histidine samples were also crystallized in the presence of 0.5 mol % CuCl₂ to reduce the proton spin–lattice relaxation times.³⁷ The polymorphs were confirmed by X-ray powder diffraction using a Philips Analytical XPERT X-ray diffractometer, with a Cu Kα source (1.5418 Å, polarization fraction 0.500), 2θ range 5–50°, continuous scan mode, step size 0.02–0.05 deg/s. Powder patterns were simulated using the Cerius² 3.8 diffraction-crystal module.³⁸

¹⁵N NMR Experiments. ¹⁵N NMR spectra were taken on a Chemagnetics CMX400 NMR spectrometer operating at 40.18 MHz for ¹⁵N and 396.469 MHz for ¹H, and a Bruker DSX 300 spectrometer operating at 30.412 MHz for ¹⁵N and 300.132 MHz for ¹H. Cross-polarization was used with a contact time of 3 ms, 90° pulse of 5.9 μs (Chemagnetics) and 5.4 μs (Bruker) for protons, and an acquisition time of 25 ms. Recycle delays of 3 s or longer were used and 10000–30000 transients were accumulated for low spinning speed spectra. All spectra were recorded at room temperature, except that for His-Leu which was recorded at 50 °C, and all were referenced using external ¹⁵NH₄Cl, setting the ammonium peak to be 35.9 ppm downfield from that of liquid ammonia at –50 °C.

CSA Simulations. The principal values of the chemical shift tensors were extracted by computer simulation of the spectrum using the algorithm developed by Herzfeld and Berger³⁹ and a minimization routine based on the CERN-Minuit programs. The simulation program was kindly provided by R. G. Griffin. Error bars were estimated by repetition of the experiments and simulations for two or more different spinning speeds, and taking the maximum deviation from the average tensor values.

(29) Madden, J. J.; L., M. E.; Seeman, N. C. *Acta Crystallogr.* **1972**, B28, 2382–2398.

(30) Lehmann, M. S.; Koetzle, T. F.; Hamilton, W. C. *Int. J. Pept. Protein Res.* **1972**, 4, 229.

(31) Bennett, I.; Davidson, A. G. H.; Harding, M. M.; Morelle, I. *Acta Crystallogr.* **1970**, B26, 1722–1729.

(32) Román, P.; Gutiérrez-Zorrilla, J. M.; Luque, A.; Vegas, A. *J. Crystallogr. Spectrosc. Res.* **1987**, 17, 585–595.

(33) Fuess, H.; Hohlwein, D.; Mason, S. A. *Acta Crystallogr.* **1977**, B33, 654–659.

(34) Prabu, M. M.; Nagendra, H. G.; Suresh, S.; Vijayan, M. *J. Biomol. Struct. Dyn.* **1996**, 14, 387–392.

(35) Steiner, T. *Acta Crystallogr.* **1996**, C52, 2266–2269.

(36) Suresh, S.; Vijayan, M. *Acta Crystallogr.* **1996**, B52, 876–881.

(37) Hirasawa, R.; Kon, H. *J. Chem. Phys.* **1972**, 56, 4467–4474.

(38) MSI. *Cerius2*, 3.8 ed.; Molecular Simulations Inc.: San Diego, CA, 1998.

(39) Herzfeld, J.; Berger, E. *J. Chem. Phys.* **1980**, 73, 6021–6030.

¹⁵N CSA Calculations. Ab initio calculations of ¹⁵N CSA values for both neutral and cationic imidazole acetate were performed on an IBM/RS6000 Model 3CT workstation using Gaussian94⁴⁰ for geometry optimization and gauge including atomic orbital (GIAO)⁴¹ shielding calculations. The geometry was optimized using a standard 6-31G(d,p) basis set and density functional theory (DFT), employing the hybrid Becke's three-parameter functional (B3LYP).⁴² Shielding calculations were performed using a 6-311++G(d,p) basis set at Hartree–Fock and DFT-B3LYP levels. Shielding computations were also performed using the sum-over-states density functional perturbation theory (SOS-DFPT) of Malkin et. al.,⁴³ as employed in the deMon program.⁴⁴ An IGLO-III basis was used for the SOS-DFPT calculations. The model was built from the coordinates for imidazolium hydrogen maleate (CSD reference code IMZMAL11). The imidazolium and the hydrogen-bonded carboxylate group were used from this structure; the rest of the maleate was replaced by a methyl group at the α position. A linear N–H···O angle was used as observed in the imidazolium hydrogen maleate crystal structure. ¹⁵N CSA values were calculated for N···O distances set to 2.51, 2.61, 2.81, and 3.01 Å, for both the cationic and neutral species.

Results and Discussion

We have studied cationic and neutral species of the imidazole group in histidine-containing peptides using nitrogen NMR. Commonly the imidazole ring can adopt three protonation states: the protonated, cationic state (imidazolium), and two possible neutral states with different tautomeric forms (Figure 1, bottom). Under strongly basic conditions, a deprotonated or anionic imidazolate can also be formed.¹ The chemical shift tensors and isotropic shifts of the imidazole ring nitrogens for a variety of crystalline histidine-containing samples and peptides are listed in Table 1. The hydrogen-bonding partners for protonated nitrogens are generally carboxylate groups, except

(40) Frisch, M. J.; Trucks, G. W.; Schlegel, H. B.; Gill, P. M. W.; Johnson, B. G.; Robb, M. A.; Cheeseman, J. R.; Keith, T.; Petersson, G. A.; Montgomery, J. A.; Raghavachari, K.; Al-Laham, M. A.; Zakrzewski, V. G.; Ortiz, J. V.; Foresman, J. B.; Peng, C. Y.; Ayala, P. Y.; Chen, W.; Wong, M. W.; Andres, J. L.; Replogle, E. S.; Gomperts, R.; Martin, R. L.; Fox, D. J.; Binkley, J. S.; Defrees, D. J.; Baker, J.; Stewart, J. P.; Head-Gordon, M.; Gonzalez, C.; Pople, J. A. *Gaussian 94*, Revision C.2; Gaussian: Pittsburgh, PA, 1995.

(41) Ditchfield, R. *J. Chem. Phys.* **1972**, 56, 5688–5691.

(42) Becke, A. D. *J. Chem. Phys.* **1993**, 98, 5648–5652.

(43) Malkin, V. G.; Malkina, O. L.; Casida, M. E.; Salahub, D. R. *J. Am. Chem. Soc.* **1994**, 116, 5898–5908.

(44) Malkin, V. G.; Malkina, O. L.; Eriksson, L. A.; Salahub, D. R. In *Modern Density Functional Theory: a Tool for Chemistry*; Seminario, J. M., Politzer, P., Eds.; Elsevier: Amsterdam, 1995; pp 273–347.

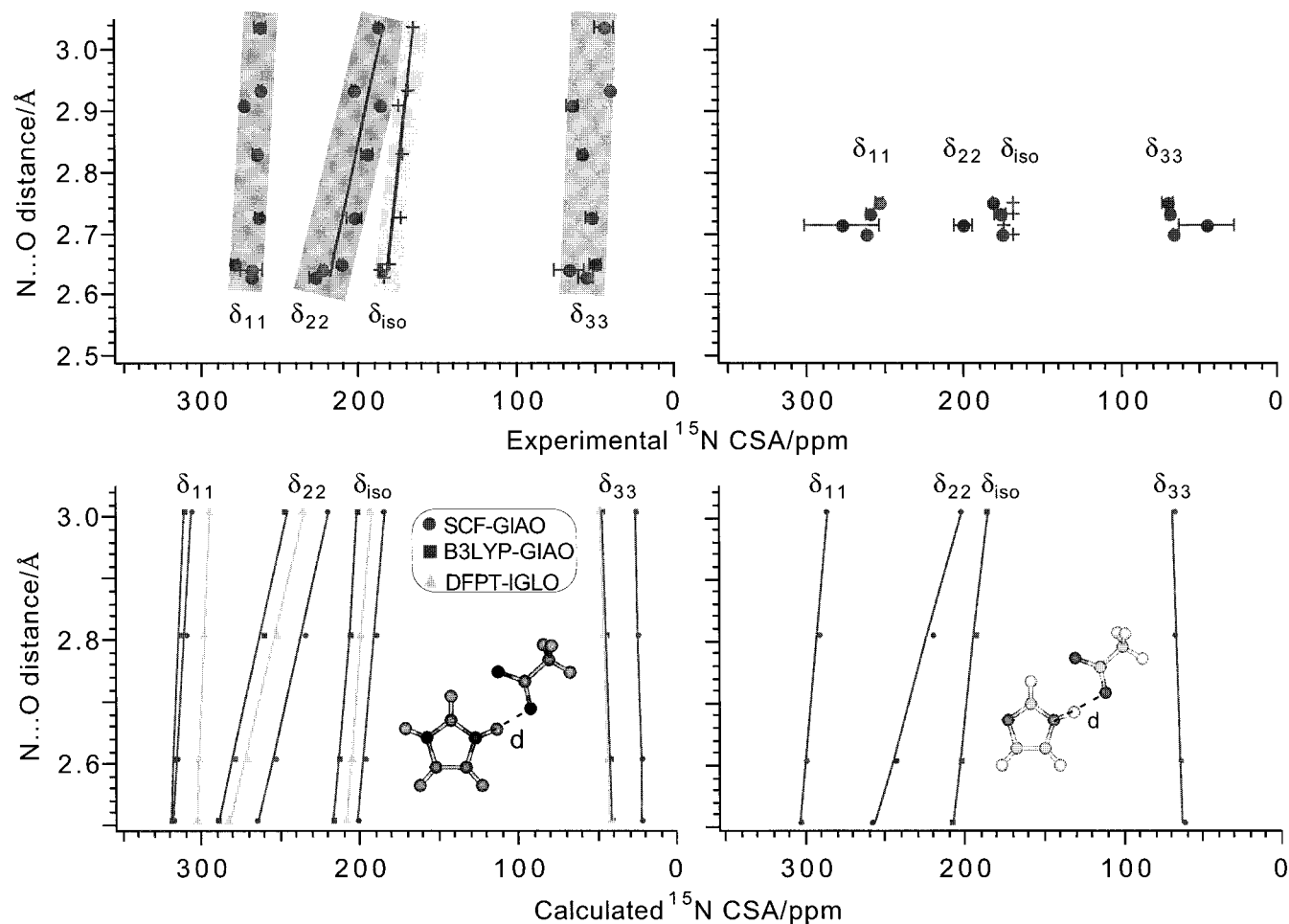


Figure 2. Experimental and calculated ^{15}N CSA tensor values for protonated imidazole ring nitrogens plotted against the N...O distances. Top: Experimental results for cationic (left) and neutral species (right). The chemical shifts were referenced using external $^{15}\text{NH}_4\text{Cl}$, setting the ammonium peak to be 35.9 ppm downfield from that of liquid ammonia at -50°C . A correlation is observed for δ_{22} for the cationic species. The error in the isotropic shift is less than 0.6 ppm, and the errors for anisotropic shifts are normally less than 5 ppm, but for some samples, the errors can be as large as 9 ppm. Circles represent anisotropic shifts, and crosses represent isotropic shifts. Bottom: Ab initio calculation results for cationic (left) and neutral species (right). The calculated chemical shifts were converted by setting the absolute shielding value of liquid ammonia at -50°C , which is 241.86 ppm, to be zero. Calculations for cationic imidazole were performed with SCF-GIAO, B3LYP-GIAO, and DFPT-IGLO methods. Calculations for neutral imidazole were done with only the DFPT-IGLO method. The models used in the calculations are also shown in plots c and d.

those listed explicitly in the table; those for deprotonated nitrogens are always amine groups ($-\text{NH}_3^+$). Donor-acceptor distances are also listed. The chemical shift values are relative to liquid ammonia at -50°C , with positive values downfield.

A dramatic difference is seen for the protonated vs deprotonated groups. The isotropic chemical shifts for deprotonated nitrogens are much more deshielded than those for protonated ones. The breadths of CSA are also much larger. For neutral species, the breadths of the tensors for deprotonated nitrogens are much greater than for the nitrogens, as described previously.¹⁹ δ_{11} and δ_{22} tensor values for deprotonated nitrogens are larger than those for protonated ones, while δ_{33} tensors are smaller (except for the case of L-His-L-Leu, whose deprotonated nitrogen (N^{c}) δ_{33} value is larger than the protonated nitrogen (N^{d}) δ_{33} tensor, presumably because it is a different tautomer than the others).

The protonated nitrogens also differ systematically (although subtly) for the cationic imidazolium species as compared with the neutral imidazole; on the other hand, we could not detect any statistically significant differences between the tensor values for the N^{c} and the N^{d} of the imidazolium; these points are discussed further below. The CSA tensors are apparently more sensitive to the environment than isotropic shifts. For example,

Table 2. Comparison of CSA Tensor Values (ppm) for L-Histidine Hydrochloride Monohydrate

N^{d}				N^{c}				
δ_{iso}	δ_{11}	δ_{22}	δ_{33}	δ_{iso}	δ_{11}	δ_{22}	δ_{33}	ref
187.0	281.7	219.3	60.0	173.4	272.5	191.3	56.3	10
186.1	272.8	217.4	68.1					11
177	257	200	74					12
185.9	268.6	222.8	66.3	172.3	265.0	195.0	58.4	this study

the isotropic shifts for monoclinic and orthorhombic L-histidine are almost identical, varying by only 0.2 ppm for both protonated and deprotonated nitrogens. However, the CSA tensor values differ by as much as 6.5 ppm for protonated nitrogen and 30 ppm for deprotonated nitrogen, making the two polymorphs of neutral L-histidine distinguishable, although we do not understand the origin of this difference yet. One entry in our table has been characterized previously. ^{15}N CSA for L-histidine hydrochloride monohydrate has been characterized by a variety of techniques. The CSA tensor values from different studies are compared in Table 2. All the chemical shift values from references were converted by setting that of liquid ammonia at -50°C to be 0 ppm. Our data are in general agreement with previous studies.

Table 3. Theoretical Calculations on ¹⁵N CSA (ppm) for Imidazolium (Cationic) Acetate

N···O distance/Å	SCF-GIAO				B3LYP-GIAO				DFPT-IGLO-III			
	δ _{iso}	δ ₁₁	δ ₂₂	δ ₃₃	δ _{iso}	δ ₁₁	δ ₂₂	δ ₃₃	δ _{iso}	δ ₁₁	δ ₂₂	δ ₃₃
2.51	201.92	318.65	265.24	21.87	217.06	319.70	290.37	41.12	209.16	303.42	282.43	41.63
2.61	197.32	315.30	253.75	22.91	213.08	317.58	279.02	42.63	205.23	301.27	271.06	43.36
2.81	189.96	310.20	234.96	24.67	206.60	313.94	260.84	45.01	198.70	297.68	252.27	46.16
3.01	184.45	306.59	220.60	26.16	201.62	311.00	247.05	46.82	192.93	294.89	235.67	48.21

To examine the dependence of CSA tensors on hydrogen-bonding distances, plots of isotropic shifts and anisotropic tensor elements as a function of hydrogen-bonding donor-acceptor distances for protonated nitrogens (N–H···O) were prepared for both cationic species. Data for the imidazolium compounds are displayed in Figure 2 (top left); data for both δ and ε nitrogens are plotted together since we could not discern a statistically significant distinction between the two classes. Data for the neutral species are also displayed in Figure 2 (top right). Circles represent the anisotropic shifts, and crosses represent isotropic shifts. The datum for DL-histidine hydrochloride dihydrate δ-nitrogen is not included in the plot, since the hydrogen-bonding partner is a chloride ion, not an oxygen atom; otherwise all data for δ and ε nitrogens were included. For DL-histidine hydrochloride dihydrate, the hydrogen-bonding distances for the two ring nitrogens differ by almost 0.4 Å, but the NMR resonances are not resolved for the two nitrogens. This apparent discrepancy may be attributed to the differences in the size and nature of the oxygen atom and chloride ion as hydrogen-bonding acceptor.

For protonated nitrogens, values for the δ₂₂ tensor element vary by 45 ppm, while those for the δ₁₁ and δ₃₃ tensor elements vary by only 20–30 ppm. A linear correlation can be found between the δ₂₂ tensor values and the hydrogen-bonding distances for cationic species: the shorter the distances, the less shielded are the δ₂₂ tensor values ($R^2 = 0.74$). The isotropic shifts for cationic species also are linearly correlated with hydrogen-bonding distances ($R^2 = 0.83$), but the range of the isotropic shifts is narrower (15 ppm). This observation provides strong motivation for using the anisotropic shift as an indicator of hydrogen bonding. The δ₁₁ and δ₃₃ tensor values are apparently not very sensitive to hydrogen bonding ($R^2 = 0.27$ and 0.20, respectively). For compounds with long hydrogen-bonding distance (N···O distance larger than 2.9 Å), bifurcated hydrogen-bonding patterns are common, which complicates the analysis. The variation in δ₂₂ (but not δ₁₁ or δ₃₃) with respect to changes in hydrogen bonding far exceeds the typical error in the points. The errors in the determination of the tensor elements are mostly <5 ppm (the errors were calculated on the basis of two or more measurements on the same sample). No substantial difference in terms of typical error values was typically found among the three tensor elements, with the exception of the data for L-His-L-Leu, which were characterized by a lower signal-to-noise ratio, and errors of 20 ppm. Thus, we conclude that for the imidazolium group the ¹⁵N isotropic shift varies systematically in response to hydrogen-bonding interactions principally because of variation in δ₂₂.

Neutral histidine residues, although often important in enzymatic catalysis, appear to have less interesting variation in hydrogen bonding in small molecules (~0.05 Å). The ranges of δ₁₁ and δ₃₃ tensor values for neutral species are similar to those of cationic species (260–280 ppm for δ₁₁ and 45–70 ppm for δ₃₃ tensors), while δ₂₂ tensor values (176–200 ppm for neutral species, 185–230 ppm for cationic species) and isotropic chemical shifts (168–175 ppm for neutral species, 172–186 ppm for cationic species) are different. For this reason separate

Table 4. Theoretical Calculations on ¹⁵N CSA (ppm) for Imidazole (Neutral) Acetate (DFPT Shielding Calculation with IGLO-III Basis Set)

N···O distance/Å	¹⁵ N			
	δ _{iso}	δ ₁₁	δ ₂₂	δ ₃₃
2.51	208.09	303.55	258.67	62.07
2.61	202.54	299.19	243.73	64.71
2.81	192.94	291.39	220.08	67.37
3.01	185.82	286.29	203.02	68.14

plots were prepared for the neutral and the cationic species. The L-His-L-Leu dipeptide was found in a N^δ–H tautomeric form as indicated by the crystal structure, while all others were in a N^ε–H tautomeric form. Although the data for this compound are poorer than those for the others, we include it here because this compound apparently does not follow the trends as observed for the more favorable N^ε–H tautomeric form. These data suggest that the δ₃₃ is greater for N^ε than N^δ, while δ₁₁ and δ₂₂ are greater for the neutral species as compared with the cationic species. Such a conclusion is weak due to the fact that our data for neutral histidines are limited; few neutral histidine structures are reported in the CSD. We do not have enough data for the deprotonated imidazole nitrogens to achieve a convincing analysis either. Not only are the data few in number, but more importantly the hydrogen-bonding distance appears to be fixed among the compounds. For the neutral imidazole motif, the pK_a match between the hydrogen bond donor and acceptor is poor, so the imidazole may be less polarizable, and apparently exhibits more fixed preferences in hydrogen-bonding lengths.

To rationalize the chemical shifts for histidine, and particularly to confirm the trends with respect to hydrogen bonding, ab initio chemical shielding calculations were performed as a function of hydrogen-bonding distance. The ¹⁵N CSA tensor values calculated for cationic species are tabulated in Table 3, and those for neutral species are listed in Table 4 (DFPT-IGLO only). Plots of ¹⁵N CSA against N···O distances are shown in Figure 2 for both cationic species (bottom left) and neutral species (bottom right). The models used for the calculations are also shown in the plots. The chemical shift values for ¹⁵N were obtained by subtracting the calculated shielding values from the absolute chemical shielding of liquid ammonia at –50 °C, which is 241.86 ppm (converted from neat nitromethane, whose absolute shielding value is –135.0 ppm⁴⁵). In other words, we report absolute shifts on a standard parts per million scale. In the calculations for cationic species, the DFPT-IGLO method gave the closest agreement for the CSA tensor breadth (δ₁₁–δ₃₃) as compared to experiment. The three methods yield similar slopes, and the only difference is in their absolute values or offset. For these reasons, only the DFPT method was used in calculating neutral species. In the calculations, the differences between cationic and neutral species are reproduced very well; i.e., the outer tensor elements are similar for the cation and the neutral species while the middle tensor element and the isotropic shift have a systematic offset. The absolute chemical shifts are

(45) Mason, J. *Multinuclear NMR*, 1st ed.; Plenum Press: New York, 1987; p 639.

Table 5. Orientations of Calculated ^{15}N Shielding Tensors of Protonated Nitrogen in Imidazole

	angle of the principal axis system			direction cosine of the principal axis system		
	<i>x</i>	<i>y</i>	<i>z</i>	<i>x</i>	<i>y</i>	<i>z</i>
δ_{11}	168.07	101.941	90.0745	-0.9784	-0.2069	-0.0013
δ_{22}	78.0593	168.07	90.0802	.2069	-0.9784	-0.0014
δ_{33}	90.0573	90.0917	0	-0.0010	-0.0016	1.0000

also in good agreement with experimental values. The calculated CSA tensors have a breadth of about 260 (DFPT-IGLO) to 300 (SCF-GIAO) ppm, which is larger than the experimental values, whose typical breadth is 200–240 ppm. The reason for overestimation of the tensor breadth may be simplifications in the model fragment used in the calculations: only an acetate counterion is included in the model. Additional interactions in the real environment would be expected to reduce the tensor breadth. The tensor orientations were also obtained through ab initio calculations. The most shielded component, δ_{33} , is normal to the imidazole plane, the most deshielded tensor, δ_{11} , lies in the plane and about 12° from the N–H bond, and the other tensor, δ_{22} , which is most sensitive to hydrogen bonding, also lies in the plane, but perpendicular to the N–H vector. The calculated angles and direction cosines of the principal axis system of the ^{15}N shielding tensor of the protonated nitrogen in the imidazole ring are collected in Table 5; the laboratory frame has the *x*-axis collinear with the N–H vector and the imidazole molecule lying on the *xy* plane. The calculated orientations are in good agreement with previous experiments.^{10,12}

More importantly, the calculations qualitatively reproduce the trend in the ^{15}N δ_{22} tensor element and isotropic shifts for the imidazolium group: the longer the N \cdots O distance, the more shielded the δ_{22} tensor values and isotropic shifts. For studies of the δ_{33} or δ_{11} tensor elements, the scatter in the experimental data is of the same magnitude as the observed trend, making the comparison of experiments with calculations insignificant. In the calculated CSA tensors for the cationic species, δ_{22} values have the largest variation, up to 45 ppm, which also reproduces the experimental results. In contrast, the other two tensors vary by about 5–10 ppm, and the isotropic shifts vary by about 16.2 ppm (DFPT-IGLO), while hydrogen bond distance varies in the range of 2.5–3.0 Å. Such a range of variation is somewhat smaller than for experimental results (which vary about 20–30 ppm for δ_{11} and δ_{33} elements and 20 ppm for isotropic shifts in the range of 2.6–3.0 Å).

The comparison of calculated and measured hydrogen-bonding trends for the CSA of the neutral histidine species is less clear. In the calculation, the ^{15}N isotropic shift changes by 22.3 ppm (DFPT-IGLO) as the hydrogen-bonding distances vary from 2.5 to 3.0 Å. The δ_{22} element is most sensitive, varying by 55.6 ppm in the same range of hydrogen-bonding distance. The ranges of variation for δ_{11} and δ_{33} elements are 6.1 and 17.3 ppm, respectively. The experimental data show that the ^{15}N chemical shift decreases with increases in the hydrogen bond length, and the δ_{22} tensor element seems to be most sensitive. The δ_{33} tensor element also exhibits some dependence on hydrogen-bonding distance according to the calculations, but the experimental data are probably too few and too noisy to allow for comparison. The δ_{11} tensor element is not sensitive to hydrogen-bonding distance. It is not possible to confirm these trends at present since the well-characterized crystalline solids

involve a nearly fixed hydrogen bond length, and we have been so far unsuccessful in preparing compounds with more interesting hydrogen-bonding motifs.

These data confirm many findings from the previous literature. The orientation of the tensor in the molecular frame is in excellent agreement with that determined experimentally (within 5°). The trends for δ_{iso} with respect to hydrogen bond strength that were hypothesized previously are indeed supported by this study.^{4,5} The absolute values for δ_{iso} also support the hypothesis that a relatively short hydrogen bond is formed between the active site imidazolium and the carboxylate functionalities in α -lytic protease under acidic conditions. Although these conclusions were presented previously, our database and calculations provide clear support for such interpretations.

One new conclusion from this work is that principally one component, δ_{22} , of the chemical shift tensor is sensitive to the variation of hydrogen-bonding distance as indicated by both experiment and theoretical calculations. In analyses of cross-correlated relaxation experiments, it is often assumed that backbone amide ^{15}N CSA tensors are constant for all residues, including both tensor orientation and magnitude of principal components.^{13,46} This study shows that such an assumption is not likely to be valid for imidazole.

Another new conclusion is that the dependence of the hydrogen bond is much more apparent for near $\text{p}K_{\text{a}}$ -matched hydrogen-bonding partners (imidazolium and carboxylate) than for far mismatched cases (neutral imidazole and carboxylate). In our study the imidazolium nitrogens participate in hydrogen bonds with carboxylate groups, but a dramatic variation in hydrogen-bonding distance and nitrogen shifts is seen. On the other hand, the imidazole groups are much less variable in the preferred distances and in their NMR properties. An analogous qualitative trend is seen also in the proton NMR and carbon NMR of carboxylates, as contrasted with the carbonyl of the amide group; only those functionalities that are involved in near $\text{p}K_{\text{a}}$ -matched pairs tend to show dramatic variation in bond lengths and systematic variation in NMR shielding tensors in response to hydrogen bond lengths.

Conclusions

We have investigated hydrogen bonding of the imidazole ring and its effects on ^{15}N CSA tensor values for histidine and histidine-containing peptides. ^{15}N CSA measurements provide valuable information on the hydrogen-bonding geometry for the imidazole ring; in particular, the δ_{22} tensor value is a good indicator of hydrogen bond length in cationic imidazole species, but the neutral species exhibited a much more restricted repertoire of hydrogen-bonding lengths and NMR shifts. The other two tensor elements, δ_{11} and δ_{33} , are apparently not sensitive to the hydrogen-bonding environment. Ab initio calculations of ^{15}N CSA for cationic species are in qualitative agreement with experimental results, and reproduce the hydrogen-bonding trends seen in the experiments.

Acknowledgment. We thank the National Institute of Health (Grant NIH RO1 GM 49964) and RC COTTRELL (Grant CS 0046) for generous financial support. We are grateful to Dr. Pierre Biscaye and Dr. Adele Hanley for help with the X-ray diffraction experiments.

JA9919074

(46) Tjandra, N.; Bax, A. *J. Am. Chem. Soc.* **1997**, *119*, 8076–8082.